Effect of rhenium doping on various physical properties of single crystals of MoSe$_2$

Mihir M. Vora[1] and Aditya M. Vora[1, 2, †]

[1] Parmeshwari 165, Vijaynagar Area, Hospital Road, Bhuj–Kutch, 370001, Gujarat, India

[2] Humanities and Social Science Department, S. T. B. S. College of Diploma Engineering, Shri Swami Atmanand Sarswati Vidya Sankul, Opp. Kapodra Police Station, Varachha Road, Surat 395 006, Gujarat, India

Abstract: Effect of rhenium doping is examined in single crystals of MoSe$_2$ viz. MoRe$_{0.005}$Se$_{1.995}$, MoRe$_{0.001}$Se$_{1.999}$ and Mo$_{0.995}$Re$_{0.005}$Se$_2$, which is grown by using the direct vapor transport (DVT) technique. The grown crystals are structurally characterized by X-ray diffraction, by determining their lattice parameters *a* and *c*, and X-ray density. Also, the Hall effect and thermoelectric power (TEP) measurements show that the single crystals exhibit a p-type semiconducting nature. The direct and indirect band gap measurements are also undertaken on these semiconducting materials.

Key words: structural properties; electrical properties; optical properties; single crystals

DOI: 10.1088/1674-4926/33/1/012001   **EEACC:** 2520

1. Introduction

In the last several years transition metal dichalcogenides (TMDC) materials have received rapidly growing attention. Many compounds of this family have a layered structure and occupy a central position in the class layered compounds due to their various important applications such as solid lubricants, energy converters, semiconductors, switching devices and model substances for testing and exploring photo-emission methods. Moreover, their polytypic and anisotropic behavior in the past few years has become an intensively investigated field in the study of the solid state research. Such compounds have a general formula TX$_2$, where T is a transition metal from IV-B, V-B and VI-B group of the periodic table and X is one of the chalcogens i.e. sulfur, selenium or tellurium. The basic structure of loosely coupled X–T–X sheets make such materials extremely interesting such that within a layer, the bonds are strong, while between the layers they are remarkably weak[1−19]. Some of the TMDCs have recently found applications in the construction as an electrode in photoelectrochamical (PEC) solar cell for conversion of solar energy into electrical energy as well as photonic devices in various electronic applications. Intercalated compounds of disulphide and diselenide of molybdenum and tungsten have been extensively studied by various researchers in the literature so far[1−19]. These single crystals become superconducting when intercalated with alkali and alkaline earth metals.

Agarwal et al.[17] have reported growth conditions, growth mechanism and lattice parameters, room temperature resistivity, low temperature resistivity and thermoelectric power of the single crystal of Mo$_{0.995}$Re$_{0.005}$Se$_2$. Also, they have noted that the Seeback coefficient and Hall coefficient measurements reveal that all the samples are n-type in nature. Agarwal and Gupta[18] have reported the energetic band location of rhenium-doped MoSe$_2$ single crystals to assess their usefulness in PEC solar cell fabrication and noted that the transmission spectra show the crystals of MoSe$_2$ and rhenium-doped

MoSe$_2$ to be direct band gap semiconductors with band gaps of 1.6 and 1.2 eV, respectively. While, Hu et al.[19] have reported a chemical vapor transport (CVT) process where Br$_2$ is used as a transporting agent for growing large sized MoSe$_2$ single crystals by adding Re (rhenium) doping (nominal concentration of 1%) during the growth process. Study of the influence of crystal anisotropy on the electrical and optical properties of the layered crystals was carried out by Hu et al.[19]. It is found from the study of Hu et al.[19] that the conductivity anisotropy decreases drastically as a result of doping and the crystal anisotropy has a more pronounced influence on the indirect gap as compared to the direct gap of the layered crystal. Very recently, we have studied various optical properties of intercalated and Re-doped compounds of MoSe$_2$ single crystals[1−13].

2. Experimental details

It has now been decided to carry out the intercalation of MoSe$_2$ either by cation or by anion substitution with elements having more electrons than molybdenum. It means that the compounds will either have the formulae Mo$_{1−x}$B$_x$Se$_2$ or MoB$_x$Se$_{2−x}$, with B as the intercalating metal. For carrying out effective intercalation at the cation site with elements of groups higher than that of the molybdenum, the general rule for solubility defined by Hicks[20] has been followed. According to Hicks[20], not only must the intercalating elements have an ionic radius close to that of the host metal, but also it must come from an adjacent group of the periodic table. In the case of MoSe$_2$, two elements, 'Mn' and 'Re', are available in the group VII-B, which is the next higher group from that of molybdenum, only rhenium (Re) has appreciable solubility, apparently because its ionic radius is closer to that of molybdenum than that of manganese (Mn). Therefore, we have decided to work on Mo$_{0.995}$Re$_{0.005}$Se$_2$ compounds in the form of the single crystals as an example of intercalation at the cation site and MoRe$_{0.005}$Se$_{1.995}$ and MoRe$_{0.001}$Se$_{1.999}$ compounds

in the form of the single crystals as an example of intercalation at the anion site. Therefore, the effect of intercalation at the cation and anion sites by rhenium on the various physical properties has been thoroughly studied and discussed in this article.

Re-doped single crystals are grown by using the direct vapor transport (DVT) method inside a dual zone horizontal furnace[17, 18]. In the present case the furnace is controlled by a micro controller with thermal profile programming facility and a solid-state relay (SSR) based power unit for the two zones of the furnace with suitable back up to account for power supply issues has been used. A high quality fused quartz tube is used for crystal growth.

X-ray powder diffractograms were recorded with the help of an X-ray diffractometer using Cukα radiation. For this purpose, many small crystals from each group were finely ground with the help of agate mortar and filtered through 106 μm sieve to obtain grains of nearly equal size. The X-ray diffractograms are taken from X-ray spectrometer. Basically, it is useful to know about the structure of the single crystals and diffracting path of the X-ray from lattice cites. The X-ray diffractograms are taken from the reported data of Gupta *et al.*[17, 18].

The density of the grown crystal was calculated by[2]

$$\rho = \frac{\sum A}{N V}, \tag{1}$$

where $\sum A$, N and V are the total weight of the atom in unit cell, Avogadro's number and volume of the unit cell, respectively. The volume of the unit cell is written as[2]

$$V = \frac{\sqrt{3}}{2} a^2 c = 0.866 a^2 c. \tag{2}$$

The crystals with an irregular shape and a larger size were normally selected to investigate their electrical behavior through the Van der Pauw method[2]. This method has certain requirements related to the ohmic contacts of the sample; if the method is not followed perfectly the observed results may be associated with some error. This error will be proportional to the dimension of the contact. After reducing the error with proper contacts, the Hall effect measurement is performed by using standard apparatus. The experiment is performed by measuring the voltage across the currents between the diagonally opposite contacts under a standard electromagnet. This magnetic field modifies the path of the electrons producing the Hall voltage. By knowing the values of difference in resistance (R), magnetic field (B) and the thickness of the sample (t), the mobility of charge carriers was evaluated using the equation,

$$\mu_{\mathrm{H}} = \frac{t R}{B \rho}, \tag{3}$$

where ρ is the room temperature resistivity of the sample. The Hall coefficient and carrier concentration were calculated using the formula

$$R_{\mathrm{H}} = \mu_{\mathrm{H}} \rho, \tag{4}$$

and for carrier concentration is given by

$$P = \frac{1}{R_{\mathrm{H}}} e. \tag{5}$$

From the sign of the Hall coefficient, the nature of the charge carriers in the grown samples could be ascertained. The magnetic field used here varied from 8.79 to 13.64 kG. The Hall coefficient and carrier concentration for each samples are calculated by using Eqs. (4) and (5).

Basically, the thermoelectric power measurement provides information on the mechanism of electrical conduction when a material is subjected to a temperature gradient under a condition in which no current is drawn a thermo-electromotive force is developed between the two terminals. This phenomenon is known as the Seeback effect. Thermo power measurements of the Seeback coefficient (S) of $MoRe_{0.005}Se_{1.995}$, $MoRe_{0.001}Se_{1.999}$ and $Mo_{0.995}Re_{0.005}Se_2$ single crystals were carried out on TEP apparatus in the temperature range from room temperature to 140 °C. To measure the S of the sample used in the present investigation as a function of temperature standard differential temperature controller apparatus was used. It consists of two blocks: (1) sample holder with heaters and pick up probes; and (2) electronic circuits controlling temperature and temperature gradient across the sample. The sample holder consists of two low power heaters A and B (15 W each). Temperature T of A is measured by using a thermocouple (TC_1) and the temperature gradient ΔT between A and B is measured by using a differential temperature sensor (TC_2). Both the thermocouples are of k-type. The sample under investigation is mounted directly on the heaters and is held by two pick-up probes, which are made of copper or stainless steel. These probes are also measure the Seeback voltage developed across the two ends of the sample. With the help of such electronic control circuits, it is possible to generate a stable temperature gradient between two heaters. It is possible to control T from 298 to 573 K and ΔT to ± 10 K stability simultaneously with better than ± 1 stability. The problem usually encountered in making thermoelectric power measurements are stray choice of electro-motive forces (emfs). In the present instrument, this problem has been eliminated by providing a choice of temperature gradient in the range between 1–10 K. The sample holder and the electronic circuits have been integrated into one unit. The use of low power heaters and electronic controllers make the operation easy and the Seeback coefficient of the samples can be measured very conveniently. The thermoelectric power or Seeback coefficient S is obtained as

$$S = \Delta T \xrightarrow{\lim} 0 \frac{\Delta V}{\Delta T} = \frac{\mathrm{d}V}{\mathrm{d}T}, \tag{6}$$

where ΔV is the potential difference produced due to the temperature difference ΔT between two points.

A Back Man model DK-A spectrometer provides a means for analyzing liquids, gases and solids through the use of radiant energy in far and near UV, visible and IR regions of the electronic spectrum. Analytical information can be revealed in terms of transmittance, absorbance and energy of reflectance in the wavelength range between 160 and 3500 mill μm. This model utilizes a single beam of energy which is chopped into alternative reference and sample beam to provide a double beam system within the sample component. The sample and reference beam have common detection and amplification components. Since these crystals are semiconducting in nature, the optical characterization for determining the direct and indirect band gap is carried out on a UV–VIS–NIR spectropho-
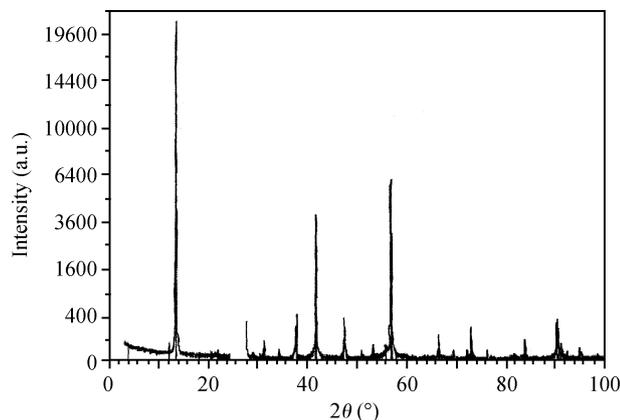
Fig. 1. X-ray diffractogram of $MoRe_{0.005}Se_{1.995}$ single crystal.
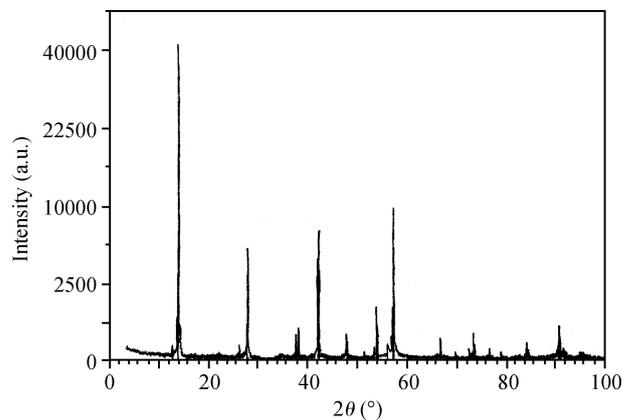
Fig. 3. X-ray diffractogram of $Mo_{0.995}Re_{0.005}Se_2$ single crystal.
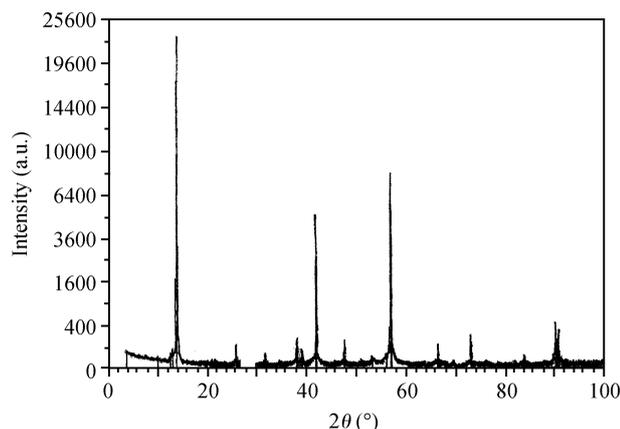
Fig. 2. X-ray diffractogram of $MoRe_{0.001}Se_{1.999}$ single crystal.
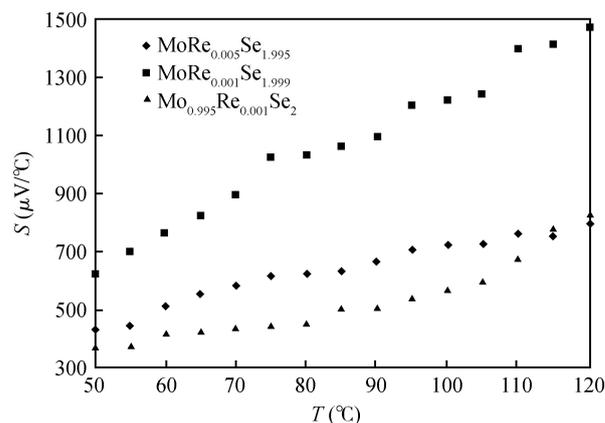
Fig. 4. Seeback coefficient (S) (μV/°C) of Re-doped $MoSe_2$ single crystals.

tometer in the range 700 to 1450 nm.

3. Results and discussion

The X-ray diffractograms and thermoelectric power or Seeback coefficient (S) of $MoRe_{0.005}Se_{1.995}$, $MoRe_{0.001}Se_{1.999}$ and $Mo_{0.995}Re_{0.005}Se_2$ single crystals are displayed in Figs. 1–4. While, the values of lattice parameter 'a' and 'c', volume, X-ray density obtained from the X-ray diffractograms, the Hall coefficient, the resistivity, mobility and carrier concentration of the $MoRe_{0.005}Se_{1.995}$, $MoRe_{0.001}Se_{1.999}$ and $Mo_{0.995}Re_{0.005}Se_2$ single crystals are listed in Table 1.

A comparison of Figs. 1–3 reveals that the direction patterns of the intercalated compound have a marked resemblance with the diffraction pattern of 2H-$MoSe_2$. The defecation peaks are visible as seen in the $MoSe_2$. This enables us to index the intercalated compounds on a hexagonal unit cell basis and it is possible to assign index nearly all peaks in the diffractograms. A study of the X-ray diffractograms shown in Figs. 1–3 reveals the following features: (1) for each sample, the (002) reflection is of the maximum intensity and thereby indicates strong orientation along the c-axis, (2) the intensity of nearly all (101) reflections show gradually decreases with Re-content, and (3) for nearly all (001) reflections, the intensity decreases and broadening increases with increase

in the Re-content. The diffractograms for $MoRe_{0.005}Se_{1.995}$, $MoRe_{0.001}Se_{1.999}$ and $Mo_{0.995}Re_{0.005}Se_2$ single crystals are similar to those of $MoSe_2$ compounds. The lattice parameter 'a' remains constants for all the samples while there is a slight amount of increase in 'c' parameter indicates that rhenium has been doping in between the layers thereby expanding the 'c' parameter. This increase is very small because the amount of rhenium doped with $MoSe_2$ is also lesser in proportion. As the proportion of rhenium addition is increased in $MoSe_2$, its X-ray density also increases, which can be seen from Table 1. This may be because of rhenium atoms added to the lattice of $MoSe_2$. Room temperature resistivity obtained from the Hall effect decreases by addition of rhenium, which can be correlated to the decrease in band gap. Mobility and carrier concentration also increases as the proportion of rhenium increases in $MoSe_2$ crystal, which indicates the increase in the charge carriers after doping[17, 18]. Mobility and carrier concentration are strongly dependent on the Hall coefficient. In the present case, such coefficient increases after doping, may have a large effect on the mobility and carrier concentration of presently studied single crystals. The positive sign of the Hall coefficient indicates that all the samples are p-type in nature while Agarwal *et al.*[17] have reported that all $MoRe_{0.005}Se_{1.995}$, $MoRe_{0.001}Se_{1.999}$ and $Mo_{0.995}Re_{0.005}Se_2$ single crystals are n-type in nature. This may be due to certain experimental conditions.

Table 1. Physical, structural, electrical and optical data of Re-doped $MoSe_2$ single crystals.

Parameter	$MoSe_2$	$MoRe_{0.005}Se_{1.995}$	$MoRe_{0.001}Se_{1.999}$	$Mo_{0.995}Re_{0.005}Se_2$
a (Å)	3.287	3.772	3.776	3.766
c (Å)	12.921	13.102	13.140	13.026
Volume ($Å^3$)	120.90	121.64	121.88	120.65
X-ray density (gm/cm^3)	6.972	6.8247	6.8344	6.9143
Room temperature resistivity ($\Omega \cdot cm$)	5.4577	0.1061	1.3590	0.3445
Hall coefficient (cm^3/coul.)	638.22	781.80	2594.47	546.49
Mobility (cm^3/(V·s))	117.02	7367.79	1909.08	1586.28
Carrier concentration (cm^{-3})	0.97×10^{16}	7.98×10^{16}	2.41×10^{16}	1.14×10^{16}
Direct band gap (eV)	1.47	1.45	1.425	1.50
Indirect band gap (eV)	1.195	1.215	1.125	1.10

The variation of thermoelectric power or S with temperature for $MoRe_{0.005}Se_{1.995}$, $MoRe_{0.001}Se_{1.999}$ and $Mo_{0.995}Re_{0.005}Se_2$ single crystals are shown in Fig. 4. It is observed that the samples are semiconducting in behavior and p-type in nature, which are also confirmed from Hall effect measurements. For p-type semiconductors, this effect is due to the flow of holes from high temperature end to the low temperature end, thereby, building up a negative space charge region near the high temperature end and a positive space charge region near the low temperature end. This gives rise to an electrical field or potential difference to make the net current flow zero.

The optical absorption spectra have been obtained in the range 700 to 1400 nm because the absorption edge is obtained in this region. The direct and indirect band gaps for $MoRe_{0.005}Se_{1.995}$ are obtained from the graph of $(\alpha h v)^2$ versus $h v$ and $(\alpha h v)^{1/2}$ versus $h v$. The values obtained are shown in Table 1, which shows that there is no change in the indirect band gap of $MoSe_2$ after doping of rhenium while a small variation in the direct band gap has been observed. The decrease in the band gap may be because of the impurity levels introduced due to the addition of rhenium in $MoSe_2$[1−13]. The optical data reported here is taken from our earlier references[1−13]. One possible mechanism determining the features of the energy bands may be caused by inter-layer low-energy membrane rigid phonon modes, which was demonstrated by Rybak *et al.*[21].

4. Conclusion

According the Hicks[18], the intercalating element rhenium (Re) has appreciable solubility, because its ionic radius is closer to that of molybdenum (Mo). Therefore, we have decided to work on $Mo_{0.995}Re_{0.005}Se_2$ compounds in the form of single crystals as an example of intercalation at the cation site and $MoRe_{0.005}Se_{1.995}$ and $MoRe_{0.001}Se_{1.999}$ compounds in the form of the single crystals as an example of intercalation at the anion site. Hence, the effects of intercalation at the cation and anion sites by rhenium on the various physical and chemical properties have been changed thoroughly. The analysis of accurate measurements of the physical, structural, electrical and optical properties of the presently studied single crystals have shown that rhenium doping strongly affects these properties in comparison with $MoSe_2$ single crystal. Also the Hall effect and thermoelectric power measurements show that such single crystals are p-type in nature and exhibit semicon-

ducting behavior. There is no change in the indirect band gap of $MoSe_2$ after doping of rhenium while a small variation in the direct band gap has been observed.

References

[1] Vora A M, Garg P K. Effect of Indium intercalation on various properties of $In_x MoSe_2$ ($0 \leqslant x \leqslant 1$) single crystals. Indian J Phys, 2000, 74A: 563

[2] Vora A M. Transport properties measurement of indium intercalated molybdenum diselenide single crystal. M. Phil. Dissertation, Sardar Patel University, Vallabh Vidyanagar, India, 1998

[3] Vora M M, Vora A M. Anisotropy of the optical absorption in layered single crystals. Cryst Res Tech, 2006, 41: 803

[4] Vora M M, Vora A M. Anisotropy of the optical absorption in layered single crystals of $MoRe_{0.001}Se_{1.999}$. Cryst Res Tech, 2007, 42: 50

[5] Vora M M, Vora A M. Intercalation and anisotropy of optical absorption of $MoRe_{0.005}Se_{1.995}$ single crystal. Cryst Res Tech, 2007, 42: 186

[6] Vora M M, Vora A M. Electrical properties measurements of Re doped $MoSe_2$ single crystals. The African Phys Rev, 2011, 6: 129

[7] Vora A M. Effect of indium intercalation on various properties of $MoSe_2$ single crystals. Cryst Res Tech, 2007, 42: 286

[8] Vora M M, Vora A M. Electrical properties measurements of $In_x MoSe_2$ ($0 \leqslant x \leqslant 1$) single crystal. Chalcogenide Lett, 2007, 4: 77

[9] Vora M M, Vora A M. Intrinsic stacking fault in single crystal of $In_x MoSe_2$ ($0 \leqslant x \leqslant 1$). Chalcogenide Lett, 2007, 4: 85

[10] Vora M M, Vora A M. Effect of rhenium doping on various properties of $MoSe_2$ single crystal. Chalcogenide Lett, 2007, 4: 97

[11] Vora A M. Effect of rhenium doping on various properties of $MoRe_{0.001}Se_{1.999}$ single crystal. Chalcogenide Lett, 2008, 5: 17

[12] Vora M M, Vora A M. Stacking faults in Re doped $MoSe_2$ single crystals. Chalcogenide Lett, 2008, 5: 35

[13] Vora M M, Vora A M. Effect of rhenium doping on various physical properties of single crystals of $MoSe_2$. Chalcogenide Lett, 2008, 5: 65

[14] Subba Rao G V, Schafer M W. Physics and chemistry of materials with layered structures. In: Levy F, ed. Intercalated layered materials. Vol. VI. Dordrecht: D. Reidel Publishing Company, 1979

[15] Subba Rao G V, Sunandana C S. In: Honing J M, Rao C N R, ed. Preparation and characterization of materials. London: Academic Press, 1981: 269

[16] Wooloam J A, Somoano R B. Superconducting critical fields of alkali and alkaline-earth intercalates of MoS_2. Phys Rev B, 1976, 13: 3843

[17] Agarwal M K, Patel P D, Gupta S K. Effect of doping $MoSe_2$

single crystals with rhenium. J Cryst Growth, 1993, 129: 559

[18] Agarwal M K, Gupta S K. Energetic band location of rhenium-doped MoSe$_2$ single crystals to assess their usefulness in PEC solar cell fabrication. Cryst Res Tech, 1993, 28: 567

[19] Hu S Y, Liang C H, Tiong K K, et al. Effect of Re dopant on the electrical and optical properties of MoSe$_2$ single crystals. J

Alloys Comp, 2007, 442: 249

[20] Hicks W T. Semiconducting behavior of substituted tungsten diselenide and its analogues. J Electrochem Soc, 1964, 111: 1058

[21] Rybak O, Blonskii I V, Bilyi Y M, et al. Luminescent spectra of PbI$_2$ single crystals doped by 3d-metal impurities. J Lumin, 1998, 79: 257